AIP Applied Physics Letters

Low-power write-once-read-many-times memory devices

Jianpu Wang, Feng Gao, and Neil C. Greenham

Citation: Appl. Phys. Lett. **97**, 053301 (2010); doi: 10.1063/1.3473775
View online: http://dx.doi.org/10.1063/1.3473775
View Table of Contents: http://apl.aip.org/resource/1/APPLAB/v97/i5
Published by the American Institute of Physics.

Related Articles

Nonvolatile organic write-once-read-many-times memory devices based on hexadecafluoro-copper-phthalocyanine
Appl. Phys. Lett. 100, 213303 (2012)

Nonvolatile organic write-once-read-many-times memory devices based on hexadecafluoro-copper-phthalocyanine
APL: Org. Electron. Photonics 5, 116 (2012)

Improved performance of non-volatile memory with Au-Al2O3 core-shell nanocrystals embedded in HfO2 matrix
Appl. Phys. Lett. 100, 203509 (2012)

Complementary resistive switching in tantalum oxide-based resistive memory devices
Appl. Phys. Lett. 100, 203112 (2012)

Materials for phase-change memory with elevated temperature stability
J. Appl. Phys. 111, 102808 (2012)

Additional information on Appl. Phys. Lett.

Journal Homepage: http://apl.aip.org/
Journal Information: http://apl.aip.org/about/about_the_journal
Top downloads: http://apl.aip.org/features/most_downloaded
Information for Authors: http://apl.aip.org/authors

ADVERTISEMENT

Downloaded 23 May 2012 to 38.107.179.218. Redistribution subject to AIP license or copyright; see http://apl.aip.org/about/rights_and_permissions

Low-power write-once-read-many-times memory devices

Jianpu Wang,[a)] Feng Gao, and Neil C. Greenham
Cavendish Laboratory, J. J. Thomson Avenue, Cambridge CB3 0HE, United Kingdom

(Received 2 April 2010; accepted 29 June 2010; published online 2 August 2010)

We introduce low-power write-once-read-many-times memory devices fabricated from solution. These devices are based on an electron-only structure using colloidal ZnO semiconductor nanoparticles and the doped conjugated polymer polyethylenedioxythiophene doped with polystyrene sulfonic acid (PEDOT:PSS). The conductive p-doped conjugated polymer is permanently dedoped by injected electrons, producing an insulating state. This demonstration provides a class of memory devices with the potential for extremely low-cost, low-power-consumption applications, such as radio-frequency identification tags. © *2010 American Institute of Physics*. [doi:10.1063/1.3473775]

Radio frequency identification (RFID) tags are an attractive application for printed organic circuits,[1–3] especially when the circuit can be printed directly on the same substrate as the antenna used to power the circuit.[4,5] RFID tags require a memory component which can be programmed and read using the power taken from the radio frequency field. Therefore it is necessary to have very low current consumption and operating voltage. For large-volume, disposable RFID applications, write-once-read-many-times memory (WORM) is sufficient, and this can be achieved from devices based on polyethylenedioxythiophene doped with polystyrene sulfonic acid (PEDOT:PSS), a commonly used conducting polymer in the field of organic electronics. This was first demonstrated by Möller *et al.*,[6] who deposited a PEDOT:PSS thin film on a p-i-n silicon structure. High-voltage pulses and large current densities were needed to program the memory arrays. Later, Brito *et al.*[5] introduced a low-power WORM memory device in patterned microholes, but the lithography process raises the cost and restricts the applicability of this type of device. Here we demonstrate a WORM device which can be fabricated by solution processing on an ITO glass substrate. The device uses a layer of wide-bandgap colloidal semiconductor ZnO nanoparticles to inject electrons into the PEDOT:PSS. The WORM memory devices can be programmed at power densities of less than 0.1 W cm^{-2}, which is orders of magnitude lower than previously reported ultralow-power WORM devices.[5]

The memory devices described here use colloidal nanoparticles of the wide-bandgap semiconductor ZnO as a hole-blocking layer. The ZnO nanoparticles are synthesized and prepared according to a previously reported method,[7,8] with a typical diameter of 5–6 nm, and coated with *n*-butylamine ligands. To produce the device structure shown in Fig. 1, ZnO nanoparticles are spin-coated from chloroform solution onto a patterned indium-tin oxide (ITO) coated substrate, followed by annealing at 250 °C in air. A PEDOT:PSS layer is then spin-coated, before thermal evaporation of Al top electrodes. The ITO pattern is a 1×12 mm^2 stripe, and the Al pattern is 1×4.5 mm^2 stripe. The device is defined by the intersection of the two electrodes, with an area of 1×1 mm^2.

A typical current-voltage characteristic of this type of device is shown in Fig. 2(a). Positive bias corresponds to a positive voltage on the Al electrode. Scanning from −2 V toward positive voltages, the initial J-V characteristic shows rectifying behavior, with a rectification ratio of 100 at ±1 V. Scanning further into forward bias, the current density peaks between 1.2–2 V at values of less than 1 mA cm^{-2}. (The exact behavior depends on the sweep rate; see Fig. 3.) When swept back below 2 V, the current is 2–3 orders of magnitude lower than the previous current. The conductivity cannot be recovered, even by applying reverse voltages, indicating a permanent change to the device. Figure 2(b) presents the transient current response to pulses of various voltages. It shows that the conductivity has decreased significantly in about 60 ms at 3 V, with faster decay under higher bias. A single 60 ms pulse (3 V) is sufficient to reduce the conductivity subsequently measured at 1 V by two orders of magnitude. Figure 2(b) also indicates that the power density required to program the memory device can be less than

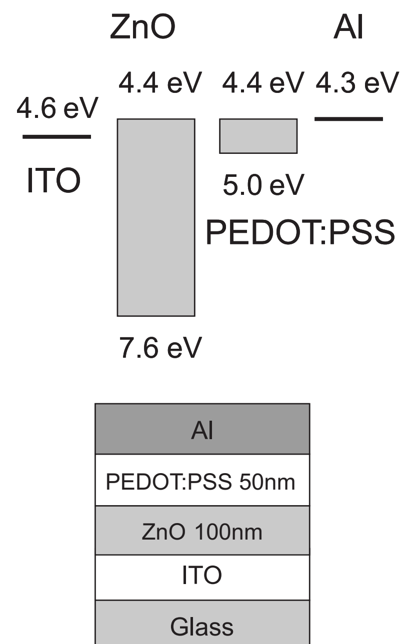

FIG. 1. Schematic device structure and energy level diagram. Energy levels are taken from Refs. 6 and 13.

a)Electronic mail: jw479@cam.ac.uk.

0003-6951/2010/97(5)/053301/3/$30.00 © 2010 American Institute of Physics

Downloaded 23 May 2012 to 38.107.179.218. Redistribution subject to AIP license or copyright; see http://apl.aip.org/about/rights_and_permissions

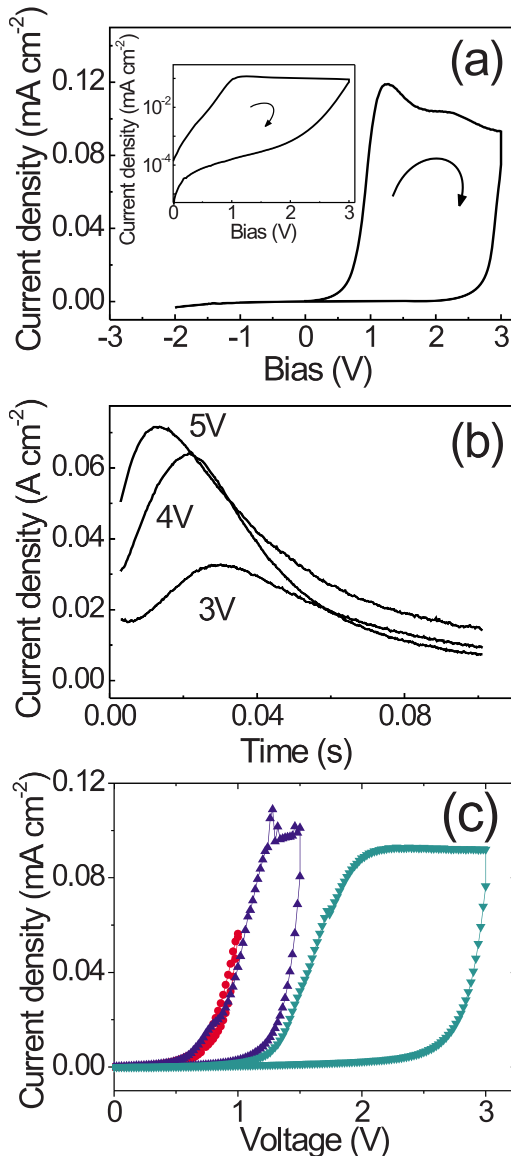

FIG. 2. (Color online) (a) Current-voltage curve for an ITO/ZnO/PEDOT:PSS/Al device. The inset shows the same data on semilogarithmic axes. (b) Current density as a function of time for devices after application of a fixed voltage. (c) Current-voltage curves for an ITO/ZnO/PEDOT:PSS/Al device measured from 0 V–1 V–0 V–1.5 V–0 V–3 V–0 V. Scan rate for (a) and (c) 0.1 V s^{-1}.

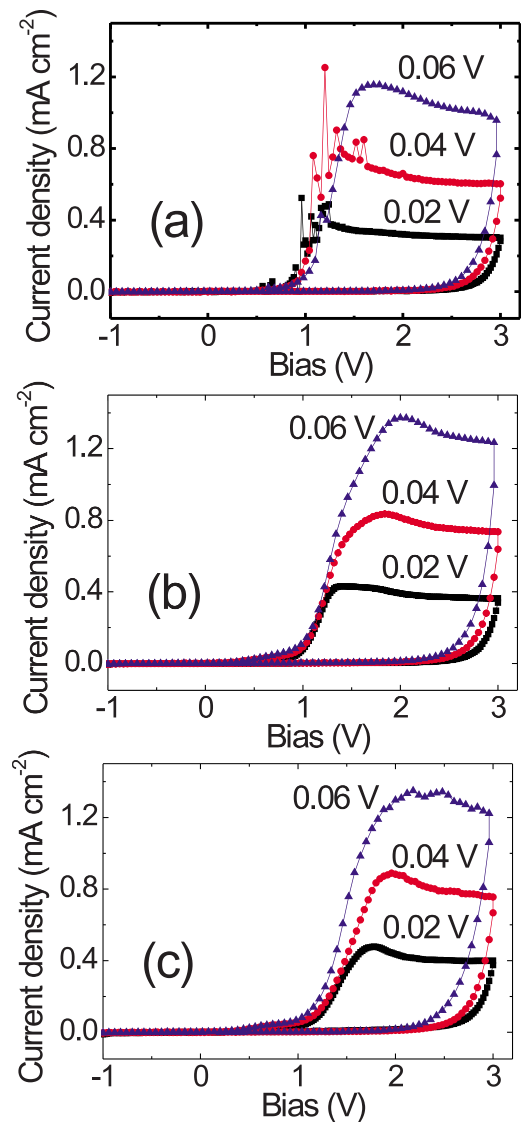

FIG. 3. (Color online) ITO/ZnO/PEDOT:PSS/Al device performance with various PEDOT:PSS layer thickness. (a) 30 nm. (b) 50 nm, and (c) 80 nm. The measurements were performed using the pulse mode of an Agilent 4155B Semiconductor Parameter Analyzer. The pulse period was 20 ms, and the pulse duration was 10 ms. Different curves denote different voltage steps (as shown in the figure) between pulses. Larger steps give higher interruption currents and voltages.

0.1 W cm^{-2}. We find the degradation of the device conductivity is small when the bias is below 1 V. Figure 2(c) shows three scans: 0 to 1.0 to 0 V, 0 to 1.5 to 0 V, and 0 to 3.0 V to 0 V in sequence with one single device. It shows that the current decreases significantly only when the bias is over 1.3 V.

A schematic energy level diagram for our device is shown in Fig. 1. We do not attempt to depict the complex band-bending that will occur close to the interfaces, the details of which will produce the observed rectifying behavior. However, the diagram is sufficient to show that hole injection is suppressed by the large ionization potential of the ZnO. Currents are therefore expected to be electron-dominated. Injection of electrons into PEDOT:PSS films is known to reduce $PEDOT^+$ to the neutral state $PEDOT^0$, thus lowering the conductivity,[9,10] and we believe this mechanism is primarily responsible for the switching in our devices. However, this mechanism alone is not sufficient to achieve the observed permanent change in conductivity, since $PEDOT^0$ can be redoped by the surrounding PSS^- when the bias is turned off. We suggest that water in the PEDOT:PSS film, which is either residual or absorbed from the atmosphere, plays an important role in the dedoping process. During switching, the PSS^- can react with the water to form stable neutral PSSH, $2PSS^- + H_2O \rightarrow 2PSSH + 1/2O_2 + 2e^-$, which results in permanent reduction in conductivity of the PEDOT:PSS film.[9,11,12] This is confirmed by experiments under a nitrogen atmosphere, where the device conductance cannot be permanently changed under such low bias.

Brito *et al.*[5] suggested that the switching mechanism in their PEDOT:PSS-based WORM devices is electrode delamination by gas formation upon electrolysis of water, and that the switching is voltage-driven. We do not believe that this is the primary switching mechanism in our devices, since the switching voltage is dependent on device thickness and sweep rate (Fig. 3). Devices with thicker PEDOT:PSS

Downloaded 23 May 2012 to 38.107.179.218. Redistribution subject to AIP license or copyright; see http://apl.aip.org/about/rights_and_permissions

layers switch at higher voltage, and faster sweep rates have a similar effect. This suggests that the switching process is more likely current-driven rather than voltage-driven. We find that a few voids are formed at the top electrode during switching, but this occurs only above 2 V, long after the dedoping process starts [Fig. 2(a)]. Electrode delamination therefore only plays a minor role. We note that the low switching currents seen in our devices are a consequence of the efficient dedoping of PEDOT:PSS by injected electrons, without the presence of a large hole current which does not contribute directly to the switching.

In summary, we have demonstrated a very low power WORM device based on ZnO nanocrystals and PEDOT:PSS. We attribute the low power of the devices due to the efficient dedoping of PEDOT:PSS by injected electrons, and the further investigation on the dedoping mechanism is in progress. Considering the low power and easy processing, our device has promising applications in plastic RFID tags.

We are grateful to Dr. Ji-Seon Kim, Dr. Jeremy Burroughes, Dr. Thomas Kugler, and Siong-Hee Khong for helpful discussions and to Cambridge Display Technology Ltd. for funding.

[1] S. Steudel, K. Myny, V. Arkhipov, C. Deibel, S. De Vusser, J. Genoe, and P. Heremans, Nature Mater. **4**, 597 (2005).
[2] Y. Noh, N. Zhao, M. Caironi, and H. Sirringhaus, Nat. Nanotechnol. **2**, 784 (2007).
[3] H. Klauk, U. Zschieschang, J. Pflaum, and M. Halik, Nature (London) **445**, 745 (2007).
[4] V. Subramanian, P. C. Chang, J. B. Lee, S. E. Molesa, and S. K. Volkman, IEEE Trans. Compon. Packag. Technol. **28**, 742 (2005).
[5] B. C. de Brito, E. Smiths, P. van Hal, T. Geuns, B. de Boer, C. Lasance, H. Gomes, and D. de Leeuw, Adv. Mater. (Weinheim, Ger.) **20**, 3750 (2008).
[6] S. Möller, C. Perlov, W. Jackson, C. Taussig, and S. R. Forrest, Nature (London) **426**, 166 (2003).
[7] C. Pacholski, A. Kornowski, and H. Weller, Angew. Chem., Int. Ed. **41**, 1188 (2002).
[8] B. Sun and H. Sirringhaus, Nano Lett. **5**, 2408 (2005).
[9] S. Möller, S. R. Forrest, C. Perlov, W. Jackson, and C. Taussig, J. Appl. Phys. **94**, 7811 (2003).
[10] J.-S. Kim, P. K. H. Ho, C. E. Murphy, N. Baynes, and R. H. Friend, Adv. Mater. (Weinheim, Ger.) **14**, 206 (2002).
[11] G. Greczynski, T. Kugler, M. Keil, W. Osikowicz, M. Fahlman, and W. Salaneck, J. Electron Spectrosc. Relat. Phenom. **121**, 1 (2001).
[12] P.-J. Chia, L. Chua, S. Sivaramakrishnan, J. Zhuo, L. Zhao, W. Sim, Y. Yeo, and P. Ho, Adv. Mater. (Weinheim, Ger.) **19**, 4202 (2007).
[13] A. Hagfeldt and M. Grätzel, Chem. Rev. (Washington, D.C.) **95**, 49 (1995).

Downloaded 23 May 2012 to 38.107.179.218. Redistribution subject to AIP license or copyright; see http://apl.aip.org/about/rights_and_permissions